ISSN 1070-4272, Russian Journal of Applied Chemistry, 2017, Vol. 90, No. 7, pp. 1068−1074. © Pleiades Publishing, Ltd., 2017.
Original Russian Text © M.A. Lapshin, R.N. Rumyantsev, A.A. Ilyin, A.P. Ilyin, A.V. Volkova, 2017, published in Zhurnal Prikladnoi Khimii, 2017, Vol. 90, No. 7, pp. 853−860.

INORGANIC SYNTHESIS AND INDUSTRIAL INORGANIC CHEMISTRY

Mechanochemical Synthesis of Highly Dispersed Iron Oxide from Metallic Powders in Manufacture of Catalysts

M. A. Lapshin, R. N. Rumyantsev, A. A. Ilyin*, A. P. Ilyin, and A. V. Volkova

Research Institute of Thermodynamics and Kinetics of Chemical Processes, Ivanovo State University of Chemical Technology, Sheremet'evskii pr. 7, Ivanovo, 153000 Russia
**e-mail: ilyin@isuct.ru*

Received August 8, 2017

Abstract—X-ray phase, X-ray diffraction, and synchronous thermal analyses, Mossbauer and IR spectroscopy, and scanning electron microscopy were used to study processes occurring in the stages of mechanochemical oxidation and thermal treatment of coarsely dispersed iron and cast iron powders in a dispersion medium of water and oxalic acid solutions. The optimal mechanochemical-synthesis conditions were determined and it was found that the preparation method affects the phase composition, structure, and properties of the resulting oxides. It was experimentally confirmed that the mechanochemical oxidation method makes it possible to obtain oxides by the zero-sewage technology with a specific surface area 1.5–12 times larger that that in oxides produced by the conventional precipitation technique. An analysis of the reactivity of the samples in the model reaction of carbon monoxide conversion by steam demonstrated their high catalytic activity.

DOI: 10.1134/S1070427217070072

The unique properties of iron oxides enable their use in various industries. The catalysis is one of their application areas. Iron oxides are catalysts and the main components in such processes as synthesis of ammonia [1], Fischer–Tropsch process [2], synthesis of toluene [3] and phenol [4], steam conversion of carbon monoxide [1, 5], partial oxidation of methanol into formaldehyde [6], dehydrogenation of methylbutenes into isoprene [7], and many others.

Highly dispersed powders of iron oxides are produced by various methods: precipitation from solutions [8], sol-gel synthesis [9], thermal decomposition (of hydroxides, nitrates, carbonates, sulfates, chlorides, alcoholates, oxalates, and other compounds of iron) [10], liquid extraction [11], microwave synthesis [12].

It is known that iron oxides used as catalysts or components of these should possess a large specific surface area and a developed porous structure and contain no noxious impurities, e.g., catalytic poisons. Therefore, certain requirements are imposed on raw materials used to produce these oxides. For example, efforts are made to avoid using iron chlorides and sulfates because chloride and sulfate ions are poisons for most of catalysts [13]. The presence of sodium is also undesirable because it can cause sintering of the finished product [14].

Of particular researchers' present interest are new alternative methods for synthesis of oxide materials and catalysts, one of which is the mechanochemical synthesis (MCS) [15, 16]. The application of this technique makes it possible to significantly simplify the technological process by diminishing the number of stages and to obtain the product without using a large amount of solvents and washing water, which minimizes the sewage formation. In addition, using the MCS method can extend the raw-material resources and yield oxide materials by using metallic powders, with the contamination possibility of the product being synthesized thereby eliminated. Analysis of published data shows that, despite the significant number of publications devoted to studies of various ways to synthesize iron oxides [8–12], the MCS is the subject of a limited number of studies [17–22], all of these being published in the last 5–10 years. For example, the authors of [18] suggest obtaining nanocrystalline wustite of nonequilibrium composition via mechanical

treatment of a $Fe + Fe_2O_3$ reaction mixture in a planetary-centrifugal mill. Lomaeva and coauthors considered [19] the process of oxidation of a pentacarbonyl iron powder in water in a planetary-centrifugal mill. In [20], it was suggested to obtain a highly dispersed iron(III) powder via joint grinding of iron chloride and sodium carbonate. The authors found that raising the grinding duration leads to a smaller particle size of the resulting Fe2O3. In [21], the phase composition and the structural parameters of a number of nanosize powders of simple ferrospinels, produced from salt systems by the method of mechanochemical reactions, were examined. There also are published data on the oxidation of a metallic-iron powder by a steam–oxygen mixture, which makes it possible to diminish the aggregation during the mechanical activation (MA) [22]. It should be noted, however, that the technology suggested by the authors of this study is difficult in implementation.

Thus, we can conclude that the research concerned with the MCS of oxide material is topical. Therefore, the goal of our study was to examine the processes of mechanochemical oxidation (MCO) of coarsely dispersed iron powders and determine their optimal parameters and also to find how a dispersion medium being used affects the phase composition, structure, and properties of the oxides being obtained.

EXPERIMENTAL

As raw materials for obtaining iron oxides served coarsely dispersed iron powders (IPs) of PZhR-3.450.26 brand (particle size up to 630 μm) and cast-iron powders (CIPs) of SCh12-28 brand (particle size up to 1250 μm). The MCO was performed in a VM-4 ring-roll vibration mill at a vibration frequency of 930 min^{-1} and provided acceleration of 3 g. The milling bodies and the working members of the mill were made of ShKh-15 steel, the milling chamber diameter was 110 mm, and the mass of milling bodies was 1194 g. As the dispersion media served water and oxalic acid solutions with concentrations of 5, 19, 15, 25, and 30 wt %. As a reference sample was used iron oxide produced by the conventional method via precipitation. The role of the starting raw material was played in this case by an iron nitrate solution. The precipitation was performed with an ammonia solution.

An X-ray phase analysis (XPA) was made with a DRON-3M diffractometer with CuKα radiation (λ = 0.15406 nm, Ni filter). The XPA data were identified by using the MINKRIST database. A thermogravimetric analysis of the mechanical-activation products was made on an STA 449 F3 Jupiter device for a synchronous thermal analysis in the At–O2 atmosphere at a heating rate of 5 deg min^{-1}. The composition of the resulting oxides and the content of metallic iron were determined by the differentiating-dissolution method based on the selective dissolution of iron from a mixture of oxides [23] and by Mossbauer spectroscopy on a YaGRS-4M spectrometer operating in the constant-acceleration mode with γ-radiation from ^{57}Co in a Cr matrix at room temperature. The surface of the samples was studied by X-ray photoelectron spectroscopy on an ES-2403 instrument with PHOIBOS-100 5-channel energy analyzer. IR spectra of the powder materials were obtained with an Avatar 360 FTIR ESP instrument in the range 400–4000 cm^{-1} in pellets with potassium bromide. The specific surface area of the samples was determined by the BET method on a Sorbi MS device. Microscopic images of the sample surface were furnished by scanning electron microscopy (SEM) on a VEGA 3 TESCAN electron microscope. The particle size distributions of the coarsely dispersed powders were determined by sieving. The amount of energy delivered in the course of MA was calculated by the procedure described in [24]. The reactivity was examined for the example of the test reaction in which carbon monoxide is subjected to a steam conversion in a PKU-2 installation under a pressure of 0.3 atm in the temperature range 250–35°C. The starting gas mixture had the following composition (vol %): CO 12, CO_2 9, H_2 55, and He the rest. The steam was proportioned to steam/gas = 1. The gas mixture was delivered to the catalyst at a volumetric flow rate of 2500 h^{-1}. The reaction products were analyzed with a Kristallyuks-4000M gas chromatograph.

RESULTS AND DISCUSSION

Analysis of the diffraction patters of the coarsely dispersed CIPs and IPs activated in water during 5–60 min shows that, prior to a thermal treatment, all the samples show broadened reflections of Fe and magnetite Fe_3O_4. The differential-oxidation method was used to demonstrate that 77.6% of CIPs and 88% of IPs is oxidized in the presence of water in the ring-roll vibration mill. Figure 1 shows Mossbauer spectra of the samples, with the corresponding distribution functions of hyperfine magnetic fields, P(H), for the as-obtained (Fig. 1a) and annealed (Fig. 1b) products formed in the MCO of cast

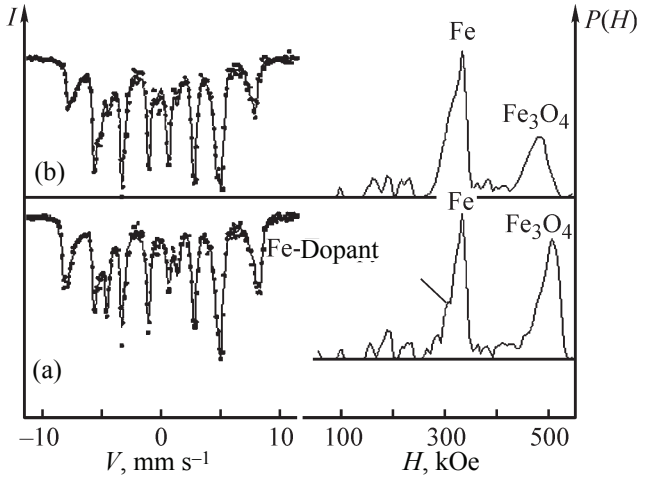

Fig. 1. Mossbauer spectra of (a) products formed in a mechanochemical oxidation of a cast-iron powder and (b) products thermally treated at 450°C for 6 h. (I) Intensity, [P(H)], distribution function of hyperfine magnetic fields, (*V*) motion velocity of the emitter, and (*H*) magnetic field strength.

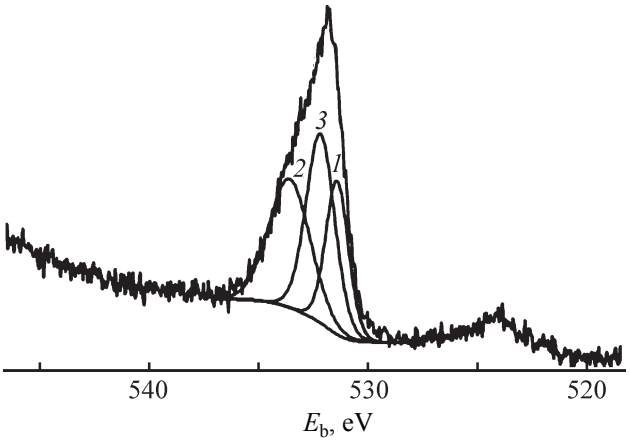

Fig. 2. 1O*s* X-ray photoelectron spectrum of products formed in MCO of CIPs with water. Binding energy E_b (eV): (*1*) FeOOH–O 530.06, (*2*) O 532.46, (*3*) FeOOH–OH 530.90.

iron in water. The types of the functions are nearly the same for both spectra. The peak positions indicate that the samples contain pure iron (333 kOe), solid-solution component (Fe as dopant) with one impurity atom in the nearest environment of an iron atom (~307 kOe) and iron oxide with nucleus-fields of ~484 kOe for the sample in Fig. 1a and 507 kOe for that in Fig. 1b. In the first sample (Fig. 1a) (with discrete processing), the shape of the "rest" component is close to that of a doublet. This indicates that there are iron clusters in the paramagnetic state, with the clusters being close in structure to hydroxides. The amount of iron atoms in this phase is 4%.

After the calcination, the amount of Fe_3O_4 is 68%, and Fe_2O_3 appears in an amount of about 10% (Table 1). With consideration for the error in determining the amount of a phase, it can be said that oxygen contained in hydroxide clusters has passed to Fe_2O_3.

A study of the surface chemical composition of a CIP sample activated in water for 60 min by X-ray photoelectron spectroscopy demonstrated (Fig. 2) that iron at the surface is in the α-FeOOH form, which corresponds to a binding energy of 711.5 eV, in agreement with published data [25]. As follows from the related models, oxygen is represented by no less than three components (Fig. 2). The states characterized by O1*s* peaks with binding energies of 530.06 and 530.9 eV belong to O^{2-} and OH^- contained in FeOOH. The oxygen form with binding energy of 532.6 eV can be rather reliably attributed to water bound on the surface [26].

The results of an X-ray diffraction analysis were used to calculate the crystal lattice constants of α-Fe to be a = 0.287 nm, in good agreement with the available published data. The value of a remains unchanged as the MA duration is raised. Hence, a conclusion can be made that, in contrast to [27], no significant amounts of oxygen and hydrogen atoms are incorporated into the iron lattice in the given case. The data we obtained agree with the results of [19]. An SEM analysis of the surface morphology (Fig. 3) demonstrated that the sample prepared by oxidation of metallic powders by water is composed of 1–15 μm flake-like aggregates with loose structure (Fig. 3a), which are, in turn, formed from finer spherical aggregates 0.2–0.4 μm in size. The micrographs of the sample produced by precipitation show that it is composed of irregularly angular aggregates with sizes of 1.5–10 μm (Fig. 3b).

A calculation of the fine crystal structure parameters of iron demonstrated that the size of coherent scattering regions (CSRs) decreases in the course of MA for samples prepared from CIPs from 28 nm after 5 min to 24 nm after 60 min, and the microstrains increase from 0.22 to 0.27% during the same time of MA. For samples prepared from IPs, the size of crystallites after 60 min of MA was 24 nm, and the microstrains were 0.32%. The size of magnetite crystallites in the final stage of MA was 22 and 19 nm for samples prepared from cast iron and iron, respectively. Iron oxide produced by the nitrate method had the following characteristics: D_{CSR} = 26 nm, microstrain ε = 0.28%.

Analysis of X-ray diffraction data shows that calcination at a temperature of 450°C for 12 h of samples

Table 1. Phase composition of products formed in MCO of CIPs in water before and after the calcination

Phase	Fraction of Fe atoms in a phase, %	Average magnetic field H on the nucleus, kOe	Isomer shift d, mm s^{-1}	Quadrupole splitting Δ, mm s^{-1}
After the MCA				
α-Fe	27	333	0.0	–
Fe_3O_4	62	451 and 486	0.66 and 0.30	–
Solid solution	7	307	0.03	0.05
The rest	4	–	–	–
After the annealing at 450°C				
α-Fe	15	333	0.0	–
Fe_3O_4	68	456 and 489	0.66 and 0.33	–
Solid solution	7	311	0.03	0.05
α-Fe_2O_3	10	517	0.37	0.10

prepared from cast iron results in that the Fe_2O_3 phase is formed and the magnetite and iron phases crystallize. In thermal treatment of samples prepared from IPs, the reflections associated with the metallic-iron phase completely disappear, and the magnetite and hematite phases crystallize. Oxidation of samples prepared from cast iron requires more severe conditions, which is due to the presence in cast iron of doping elements making slower the oxidation process. For cast iron to be fully oxidized, it is necessary to raise the time of thermal treatment at 450°C to 14 h.

The process of calcination is accompanied both by the loss of mass and by its increase (Fig. 4) It was shown that the mass of a calcined sample decreases in the temperature range 20–150°C by 1.2%, which is due to the removal of moisture and carbon dioxide, both adsorbed from air, and also to the decomposition of FeOOH. Further increase in temperature results in that the sample mass

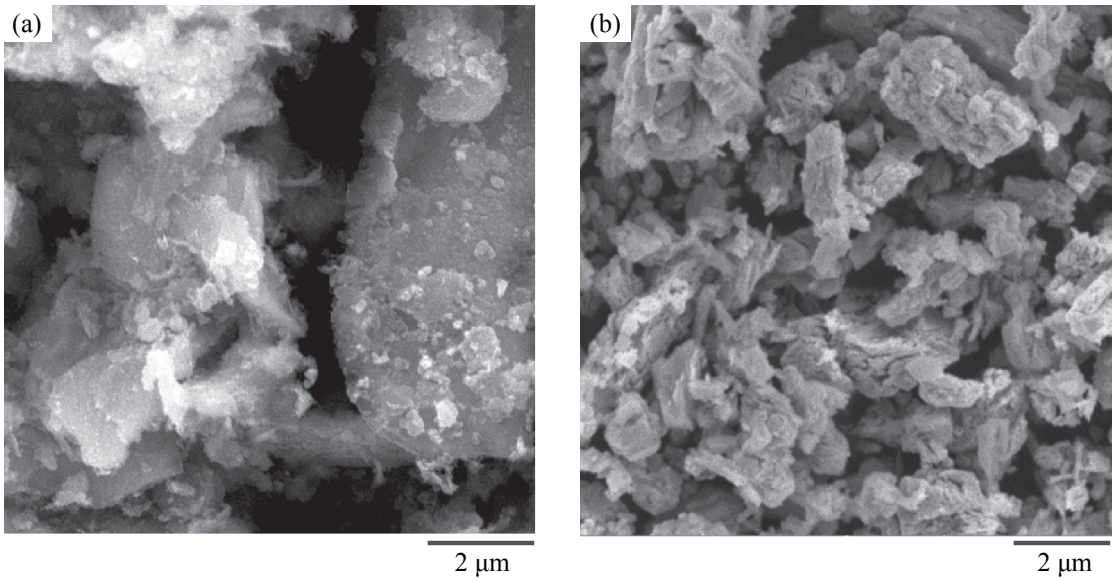

Fig. 3. SEM images of iron oxides produced by (a) MCO of a cast-iron powder with water for 60 min and (b) nitrate technology.

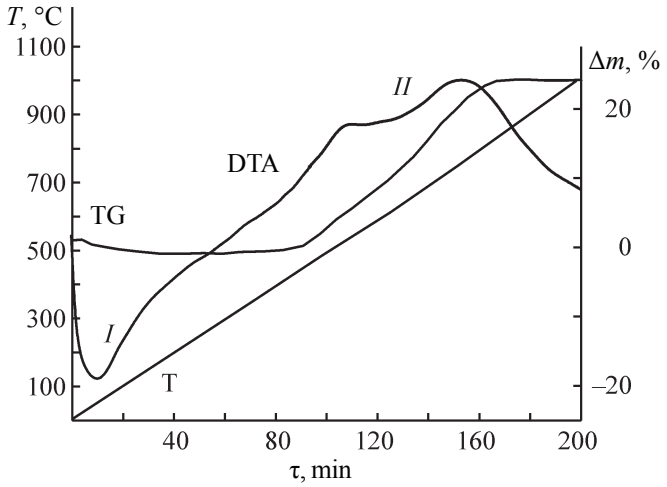

Fig. 4. Thermogram of products formed in MCO of CIPs with water. (*T*) Temperature, (Δ*m*) change in mass, (τ) time.

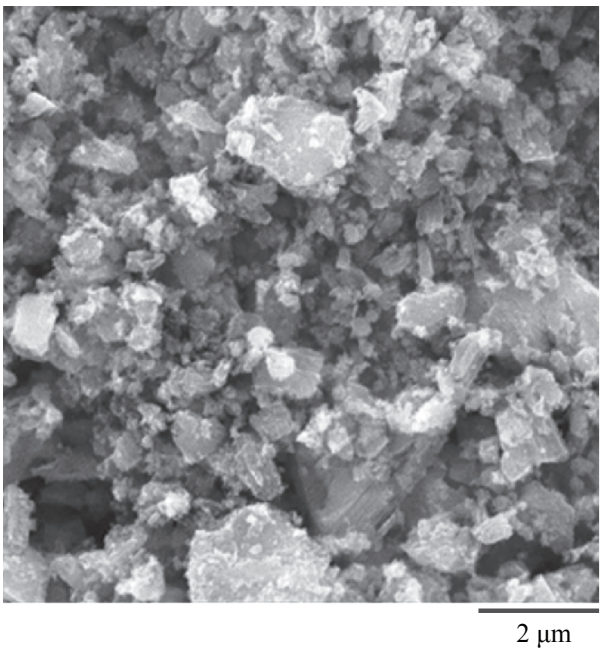

Fig. 5. SEM image of iron oxide produced by MCO of an iron powder with a 25% solution of oxalic acid: T_{treat} = 240°V.

grows. For example, upon calcination at 450 to 1000°C the sample mass increases by 24%, which is due to the oxidation of Fe^{2+} ions in magnetite and its conversion to hematite and also to the oxidation of metallic iron. The calcination process is accompanied by two heat effects: one endo- and one exothermic. Effect I in the temperature range 20–150°C is due to the removal of adsorbed water and CO_2, and also to the decomposition of FeOOH. The exothermic effect II is observed in the temperature range 500–1000°C. This effect is associated with the additional oxidation of the phases of metallic iron and the oxides. IR spectroscopic analysis of the gaseous decomposition products shows that the gas phase contains water and carbon dioxide at 20–250°C, and mostly CO_2 in the temperature range 250–310°C, with the amount of CO_2 sharply decreasing as the temperature increases further.

An analysis of the X-ray diffraction patterns obtained upon MA of iron with oxalic acid solutions demonstrated that, with acid solutions with concentrations of 5–20%, the metallic iron phase is not fully oxidized in the oxidation of IPs of CIPs. Raising the acid concentration to 25% results in that the reflection 2θ = 44.82°, characteristic of the iron phase, fully disappears. Analysis of the IR spectrum of the product obtained suggests that the state of C_2O_4 groups in the compound is close to the state of chelate (bidentately bound) oxalate groups. In particular, the IR spectrum of an uncalcined sample shows the absorption band at 1633 cm^{-1}, associated with stretching vibrations of C=O double bonds. In addition, the spectrum contains absorption bands in the range 1360–1317 cm^{-1}, which characterize antisymmetric and symmetric vibrations of C–O single bonds. To bending vibrations of C_2O_4 groups can be attributed rather strong bands in the range 1009–821 cm^{-1}. The absorption bands at 531–492 cm^{-1} are mostly associated with vibrations of Fe–O(C_2O_4). The particle size of the reaction products does not exceed 18 μm. Thus, based on the results of the X-ray diffraction analysis and IR spectroscopy, we can conclude that iron oxalate phases are present in the product, and, in addition, the reaction products may contain X-ray-amorphous substances: oxalic acid and iron oxide formed as a result of the decomposition of iron oxalate in the MA process.

Figure 5 shows a micrograph of a sample, whence it can be seen that the sample is composed of flake-like irregular aggregates with predominant sizes of 0.5–5 μm.

Calcination of the samples in air at a temperature of 240°C for 1 h yields the oxide γ-Fe_2O_3. An X-ray diffraction analysis demonstrated that, with increasing calcination temperature, the size of the CSR of the oxides being formed changes from 12 to 27 nm in the temperature range 240–450°C, with the specific surface area decreasing in the process from 120 to 70 $m^2 g^{-1}$ and the maximum size of secondary particles increasing to 28 μm. Simultaneously, there occurs recrystallization of γ-Fe_2O_3 into α-Fe_2O_3.

The IR spectra of calcined samples are rather strongly changed and indicate that anion-modified oxides are formed. The spectra of samples calcined at a

Table 2. Preparation conditions and characteristics of iron oxides

Synthesis method	τ_{MCO}, min	T_{calc}, °C	τ_{calc}, min	Phase composition	S_{sp}, m^2 g^{-1}	D_{CSR}, nm	ξ, %	CO conversion at 300°C, %
MCO:								
IP + H_2O	60	450	12	Fe_3O_4/α-Fe_2O_3	18	38/28	0.15/0.33	28.32
CIP + H_2O	60	450	14	Fe_3O_4/α-Fe_2O_3	20	34/27	0.16/0.34	29.17
CIP, 25% solution of $H_2C_2O_4$	30	240	60	γ-Fe_2O_3	123	12	0.37	42.11
		450	60	α-Fe_2O_3	77	27	0.31	35.55
IP , 25% solution of $H_2C_2O_4$	30	240	60	γ-Fe_2O_3	120	10	0.35	40.23
		450	60	α-Fe_2O_3	70	24	0.30	34.24
Precipitation (by the nitrate technology)	–	450	10	α-Fe_2O_3	12	26	0.28	24.63

temperature of 450°C show a characteristic absorption band at 1633 cm^{-1}, associated with stretching vibrations of carbonate ions. In addition, there is an absorption band at 3438 cm^{-1}, which characterizes the presence of OH^- groups.

Table 2 presents the synthesis conditions and characteristics of the oxides obtained.

To evaluate their reactivity, the oxides were tested in the reaction of steam conversion of carbon monoxide. It was found that the conversion of CO grows with increasing temperature and reaches the maximum value at 300°C. As the temperature increases further, the catalyst is sintered and, as a result, its activity sharply falls. It should be noted that iron oxides produced from CIPs possess a higher catalytic activity in all tests, compared with the oxides prepared from IPs (Table 2). Apparently, this is due to the presence in their composition of a small amount of manganese, which is a promoting agent in the given reaction [28]. The conversion of CO on oxide prepared by the MCO with an oxalic acid solution exceeds by more than a factor of 1.5 that for oxides produced by the precipitation and the MCO with water (Table 2). In all probability, this is due to the larger specific surface area and more pronounced defectiveness and dispersity.

CONCLUSIONS

(1) It was found that, in the course of a mechanochemical oxidation of iron-containing powders in water, the powders are ground and defects accumulate in the structure of iron. Simultaneously, there occur parallel processes in which iron hydroxides and the Fe3O4 phase are formed on the particle surface. Thermal treatment of the reaction products results in a dehydration of the hydroxides and an additional oxidation of the metallic-iron phase to give a double-phase system Fe_3O_4/α-Fe_2O_3.

(2) Using an aqueous solution of 25% oxalic acid as the dispersion medium can reduce the time of a mechanochemical oxidation of iron and cast iron powders to 30 min, with the presence of the metallic-iron phase upon oxidation ruled out. The thermolysis of the reaction products in the temperature range 240–450°C makes it possible to obtain both γ-Fe_2O_3 and α-Fe_2O_3, with the specific surface area of these being 70–123 m^2 g^{-1}.

(3) An evaluation of the activity of the resulting oxides in a test reaction of in which carbon monoxide is subjected to steam conversion demonstrated that iron oxides prepared via mechanical oxidation possess a higher catalytic activity, with the samples produced from cast iron powders being more reactive due to the promoting action of manganese they contain.

(4) It was confirmed that the method of mechanical oxidation can yield highly dispersed iron oxides with specific surface area exceeding by a factor 12.5–12 that of oxides prepared by the precipitation method by the nitrate technology, with the number of technological stages diminished, formation of wastewater ruled out, and amount of noxious gas discharges minimized. The high reactivity makes it possible to recommend the oxides for being used in catalysis.

ACKNOWLEDGMENTS

The study was carried out under the State assignment from the Ministry of Education and Science of the Russian Federation (project no. 3.1371.2017/4.6) with partial support by the stipend of the President of the Russian Federation for young scientists and postgraduate students carrying out promising research and development activities in priority direction of modernization of Russia's economy (2016–2018) (no. SP-3477.2016.1). The study was carried out on the scientific equipment of the Collective Use Center at the Ivanovo State University of Chemical Technology.

REFERENCES

1. Kolesnikov, I.M., *Kataliz i proizvodstvo katalizatorov* (Catalysis and Manufacture of Catalysts), Moscow: Tekhnika, 2004.
2. Park, J.Y., Lee, Y.J., Khanna, P.K., et al., *J. Mol. Catal. A: Chem*., 2010, vol. 323, nos. 1–2, pp. 84–90.
3. Miki, T. and Tai, Y., *Mater. Sci. Forum*, 2011, vol. 695, pp. 101–104.
4. di Luca, C., Massa, P., Fenoglio, R., and Cabello, F.M., *J. Chem. Technol. Biotechnol*., 2014, vol. 89, no. 8, pp. 1121–1128.
5. Khassin, A.A., Minyukova, T.P., Demeshkina, M.P., et al., *Kinet. Catal*., 2009, vol. 50, no. 6, pp. 837–850.
6. Ilyin, A.A., Rumyantsev, R.N., Zhukov, A.B., and Ilyin, A.P., *Nanotechnol. Russ*., 2016, vol. 11, nos. 9–10, pp. 569–578.
7. Karimov, E.K., Kas'yanova, L.Z., Movsumzade, E.M., et al., *Petroleum Chemistry,* 2014, vol. 54, no. 3, pp. 213–217.
8. RF Patent 2 489 358 (publ. 2012).
9. Durãesa, L., Costab, B.F.O., Vasquesa, J., et al., *Mater. Lett*., 2005, vol. 59, no. 7, pp. 859–863.
10. Rumyantsev, R.N., Ilyin, A.A., Ilyin, A.P., et al*., Izv. Vyssh. Uchebn. Zaved., Khim. Khim. Tekhnol.,* 2014, vol. 57, no. 7, pp. 80–84.
11. Kolpakova, K.E. and Sklokin, L.I., *Khim. Tekhnol*., 2001, no. 11, pp. 20–26.
12. Kulikov, F.A., Vanetsev, A.S., Murav′eva, G.P., et al., *Inorg. Mater*., 2003, vol. 39, no. 10, pp. 1074–1075.
13. *Proizvodstva ammiaka* (Ammonia Manufacture Shops), Semenov, V.P., Ed., Moscow: Khimiya, 1985.
14. Satterfield, C.N., *Mass Transfer in Heterogeneous Catalysis*, The MIT Press, 1969.
15. Ilyin, A.A., Rumyantsev, R.N., Ilyin, A.P., et al*., Russ. J. Phys. Chem. A*, 2016, vol. 90, no. 4, pp. 764–770
16. Boldyrev, V.V., Avvakumov, E.G., Boldyreva, E.V., et al., *Fundamental'nye osnovy mekhanicheskoi aktivatsii, mekhanosinteza i mekhanokhimicheskikh tekhnologii* (Foundations of Mechanical Activation, Mechanosynthesis,and Mechanochemical Technologies), Novosibirsk: Sib. Otd. Ross. Akad. Nauk, 2009.
17. Ilyin, A.A., Rumyantsev, R.N., Ilyin. A.P., et al., *Izv. Vyssh. Uchebn. Zaved., Khim. Khim. Tekhnol*., 2011, vol. 54, no. 1, pp. 103–107.
18. Emel,yanov, D.A., Korolev, K.G., Mikhailenko, M.A., et al., *Inorg. Mater*., 2004, vol. 40, no. 6, pp. 726–729.
19. Lomaeva, S.F., Maratkanova, A.N., Nemtsova, O.M., et al., *Khim. Interesakh Ustoich. Razvit*., 2007, nos. 1–2, pp. 103–109.
20. Seyedia, M., Haratiana, S., and J. Vahdati Khakia, *Proc. Mater. Sci*., 2015, no. 11, pp. 309–313.
21. Terekhova, O.G., Itin, V.I., Magaeva, A.A., et al., *Izv. Vyssh. Uchebn. Zaved., Poroshk. Metall. Funkts. Pokrytiya,* 2008, no. 1, pp. 45–50.
22. Rumyantsev, R.N., Ilyin, A.A., Ilyin, A.P., et al., *Izv. Vyssh. Uchebn. Zaved., Khim. Khim. Tekhnol.,* 2011, vol. 54, no. 3, pp. 50–53.
23. Kreshkov, A.P., *Osnovy analiticheskoi khimii* (Fundamentals of Analytical Chemistry), Moscow: Khimiya, 1976, vol. 2.
24. Heegn, H.P., *Izv. Sib. Otd. Akad. Nauk SSSR, Ser. Khim. Nauk*, 1988, issue 1, no. 2, pp. 3–9.
25. *Quantification of AES and XPS*, *Practical Surface Analysis* / Briggs, D. and Seah, M., Eds., Chichester: Wiley, 1990.
26. Grosvenor, A.P., Kobe, B.A., Biesinger, M.C., et al., *Surf. Interface Anal*., 2004, no. 36, pp. 1564–1574.
27. Cherdyntsev, V.V., Kaloshkin, S.D., and Tomilin, I.A., *Fiz. Met. Metalloved*., 1998, vol. 86, no. 6, pp. 84–89.
28. RF Patent 2 275 963 (publ. 2006).